

---

PHYSICAL METALLURGY  
AND HEAT TREATMENT

---

## Investigation of the Ni<sub>3</sub>Al–Fe Alloys by Resistivity Measurements and Differential Thermal Analysis

S. V. Lepikhin<sup>a,\*</sup> and N. N. Stepanova<sup>b,\*\*</sup>

<sup>a</sup>Ural Federal University, ul. Mira 19, Yekaterinburg, 620002 Russia

\*e-mail: lepichin@mail.ru

<sup>b</sup>Institute of Metal Physics, Ural Branch, Russian Academy of Sciences,  
ul. S. Kovalevskoi 18, Yekaterinburg, 620991 Russia

\*\*e-mail: snn@imp.uran.ru

**Abstract**—A series of iron-doped Ni<sub>3</sub>Al ternary alloys is investigated by resistivity measurements and differential thermal analysis. Temperatures of phase transformations and disordering onset are determined. A hysteresis phenomenon is observed in the liquid state in polytherms of resistivity upon heating the alloy under study to the critical temperature.

**Keywords:** Ni<sub>3</sub>Al intermetallic compound, alloying, phase transformations, disordering, melt, hysteresis, critical temperature, resistivity, differential thermal analysis

**DOI:** 10.3103/S1067821213060151

The Ni<sub>3</sub>Al-based intermetallic compound ( $\gamma'$  phase) is the main strengthening phase of foundry heat-resistant nickel alloys, which represent an important group of high-strength materials used when fabricating the most important details of gas-turbine motors [1, 2]. Currently the VKNA-type alloys based on the Ni<sub>3</sub>Al compound (90% intermetallic phase) are developed and used in industry [3].

The Ni<sub>3</sub>Al is ordered according to type  $L1_2$  and occurs in a narrow concentration range near 25 at % Al. Its feature is the ability to dissolve almost all transition elements in various combinations. Substitutional alloying of this alloy extends the occurrence region of the  $\gamma'$  phase [2] and leads to a substantial variation in the character and temperature ranges of phase and structural transformations in the Ni<sub>3</sub>Al– $X$  system [4].

Practical application as a heat-resistant construction material requires the elimination of the intercrystallite brittleness, which is inherent to the Ni<sub>3</sub>Al alloy in the polycrystalline state. Iron is considered a possible plastificator [5].

Ni<sub>3</sub>Al–Fe alloys are of interest for investigation not only from the manufacturing viewpoint, but also from the physical one. The solubility of iron in  $\gamma'$  phase substantially depends on the ratio of atomic concentrations of nickel and aluminum. The chemical activity of iron and nickel atoms is close, and iron is able to form the Ni<sub>3</sub>Fe intermetallic phase. All these factors lead to the iron atoms being able to substitute the sites of both nickel and aluminum atoms [2]. From this viewpoint, the Ni<sub>3</sub>Al–Fe system can serve as the model system for the Ni<sub>3</sub>Al-based alloyed alloys.

The Ni<sub>3</sub>Al intermetallic compound has a high degree of long-range order close to unity and retaining

upon heating to 1330°C. Above this temperature, disordering starts. The temperature of complete disordering ( $t_k$ ) is not attained in the solid state for the stoichiometric alloy (Ni<sub>75</sub>Al<sub>25</sub>). However, alloying with transition elements such as iron, chromium, and manganese promotes the transition from intermetallic properties to the properties of the ordering alloy as their concentration increases: quantity  $t_k$  can be detected in the solid state [6].

As a rule, electron scattering at lattice inhomogeneities in the solid solution decreases upon its ordering. Resistivity ( $\rho$ ) is lower in the ordered region, while a decrease in the degree of long-range order  $S$  is accompanied by an increase in  $\rho$ . For example, such dependence  $\rho(t)$  is observed for the Cu<sub>3</sub>Al ordered compound ( $L1_2$ ) [7]. On the contrary, an abrupt drop in resistivity is characteristic of the Ni<sub>3</sub>Al alloy upon decreasing  $S$  (coefficient  $d\rho/dt$  is negative. This phenomenon is observed not only for the Ni<sub>3</sub>Al ordered compound but also for some other intermetallic alloys and is associated with the features of their electronic spectrum [8].

The temperature of disordering onset ( $t_a$ ) for the Ni<sub>3</sub>Al alloy is that after which resistivity starts to decrease. If the alloy structure consists of the intermetallic compound ( $\gamma'$  phase) and the nickel-based solid solution ( $\gamma$  phase), the coincidence of dissolution of the  $\gamma'$  phase and the disordering onset is possible. Dissolution of the  $\gamma'$  phase is also accompanied by a decrease in resistivity. These processes can be distinguished by force of comparing the data of the differential thermal analysis (DTA) and the resistivity measurement: both these temperatures (i.e., the disordering onset and the dissolution of the  $\gamma'$  phase) are

Chemical composition and critical points of phase transformations on the Ni<sub>3</sub>Al–Fe intermetallic alloys

No.	Composition of the Ni–Al–Fe alloy, at %	$t_S-t_L, ^\circ\text{C}$			$t_{p. t}, ^\circ\text{C}$		$t_a, ^\circ\text{C}$	$t_k, ^\circ\text{C}$
		heating according to DTA	heating according to $\rho$	cooling according to $\rho$	heating according to DTA	heating according to $\rho$	cooling according to $\rho$	according to $\rho$
Substitution of aluminum atomic sites								
1	75–22–3	1318–1374	1325–1380	1340–1365	1200 $\gamma'\rightarrow\gamma'+\gamma$	1190 $\gamma\rightarrow\gamma'+\gamma$	1220	1780
2	75–20–5	1319–1389	1315–1390	1290–1365	716 $\gamma'\rightarrow\gamma'+\gamma$	–	1080	1745
3	75–18–7	1349–1391	1335–1405	–	721 $\gamma'\rightarrow\gamma'+\gamma$ 1172 $\gamma'\rightarrow\gamma+\gamma$	– 1190 $\gamma'+\gamma\rightarrow\gamma$	1090	–
Substitution of aluminum and nickel atomic sites simultaneously								
4	73–23–1	1317–1376	1315–1390	1290–1325	1285 $\gamma'\rightarrow\gamma+\gamma$	1275 $\gamma'\rightarrow\gamma+\gamma'$	1170	1610
5	71–21–8	1323–1367	1300–1375	–	1249 $\gamma'\rightarrow\gamma+\gamma$	1265 $\gamma'+\gamma\rightarrow\gamma'$	1005	–
Substitution of nickel atomic sites								
6	73–25–2	1317–1383	1330–1370	1305–1355	1196 $\gamma'\rightarrow\gamma'+\beta$	–	1180	1575
7	71–25–4	1321–1369	1310–1380	1285–1355	1079 $\gamma'\rightarrow\gamma'+\gamma$ 1292 $\gamma'+\gamma\rightarrow\gamma'+\gamma+\beta$ $\gamma'+\gamma+\beta\rightarrow\gamma+\beta$	1070 $\gamma\rightarrow\gamma'+\gamma$ –	1100	1640

$t_S-t_L$  are the ranges of melting and crystallization,  $t_{p, t}$  is the phase-transition temperature in the solid state,  $t_a$  and  $t_k$  are the temperatures of the disordering onset and the end for the  $\gamma'$  phase, and  $t_c$  is the critical heating temperature of the melt. Measurement accuracy of the temperature for  $\rho(t)$  is  $\pm 10^\circ\text{C}$ , for DTA  $\pm 3^\circ\text{C}$ .

present in the  $\rho$  polytherm, while only the temperature associated with the dissolution is present in the DTA curve.

The disordering onset temperature is usually not marked in phase diagrams, but for the Ni<sub>3</sub>Al-based alloys it is one of the most important characteristics which determine the working temperatures of wares.

The operational conditions make high demands for the phase and structural stability of heat-resistant alloys. An increase in stability determines the service life and operational reliability of wares made of heat-resistant alloys. One of the methods for increasing stability is the high-temperature treatment of the melt (HTTM). The HTTM essence is in heating the melt to certain temperature  $t_c$ , holding at this temperature, and subsequently cooling to the pouring temperature (after holding, the melt is discharged from the crucible). The application of the HTTM substantially affects the alloy structure in the solid state. As a result, the level of mechanical properties and the yield ratio increase [9].

We previously investigated the Ni<sub>3</sub>Al–Fe intermetallic compounds [10] and revealed several interesting regularities, but this was accompanied by the appearance of new problems. No investigation of the influ-

ence of alloying on the kinetics of ordering–disordering processes and the critical temperature in the liquid state were performed.

The purpose of this study was to determine the temperatures of phase and structural transformations in the liquid and solid states of the series of the Ni<sub>3</sub>Al–Fe alloys of various compositions in the limits of the homogeneity region of the  $\gamma'$  phase.

The samples were obtained by vacuum arc melting at the Department of Precision Metallurgy, Institute of Metal Physics, Ural Branch, Russian Academy of Sciences. According to data [11], cast polycrystalline samples were annealed at 1100°C for 100 h. The composition of studied Ni<sub>3</sub>Al–Fe alloys according to the chemical analysis data is presented in the table; in all cases it is in the limits of the homogeneity region of the  $\gamma'$  phase by the isothermal section at 1100°C presented in [2].

The temperature dependences of resistivity are obtained by a contactless method [12]. The features associated with ordering processes appear in curves  $\rho(t)$  at high temperatures. Therefore, measurements of  $\rho(t)$  are performed in a range from 900°C and above, including the liquid state.

Differential thermal analysis was performed using a VDTA-8M3 modernized differential thermal analyzer

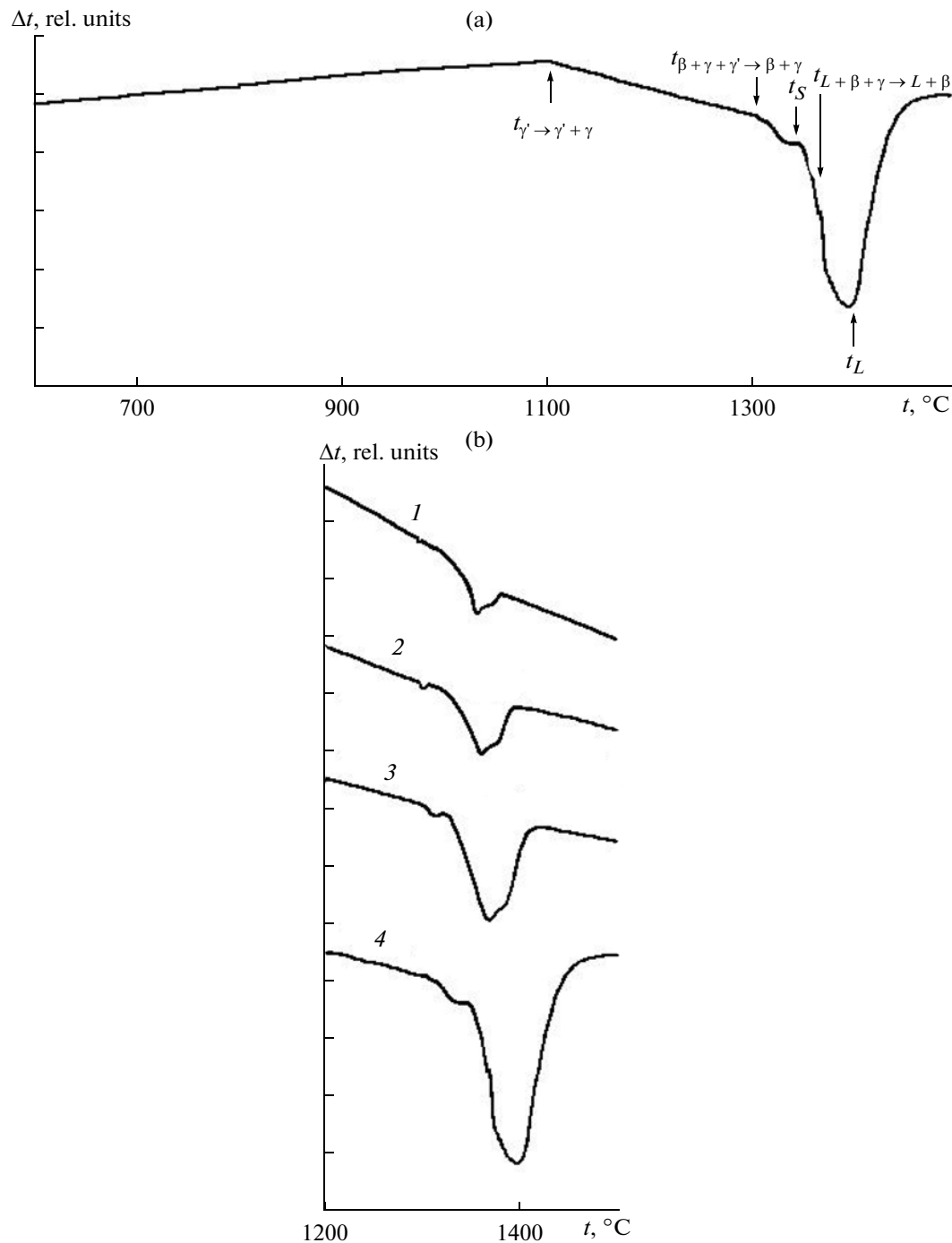


**Fig. 1.** DTA curves of the Ni<sub>71</sub>Al<sub>25</sub>Fe<sub>4</sub> alloy at various heating rates. (a)  $V = 80$  K/min, (b) = (1) 10, (2) 20, (3) 40, and (4) 80 K/min.

upon heating with rates  $V = 20, 40$ , and  $80$  K/min. To find transition temperatures which correspond to equilibrium ones, we extrapolated the results to the rate of  $0$  K/min [13].

Temperatures of phase transitions marked both in the DTA and resistivity curves are tabulated. The data of both methods agree well.

For example, Fig. 1a shows the DTA curve of the Ni<sub>71</sub>Al<sub>25</sub>Fe<sub>4</sub> alloy recorded at  $V = 80$  K/min. It should be noted that the higher the heating rate is, the larger overheating is. The DTA curves for various heating rates are shown in Fig. 1b. The higher recording rates increase the sensitivity of the method, which makes it possible to reveal the weakly pronounced transitions (Fig. 1b).

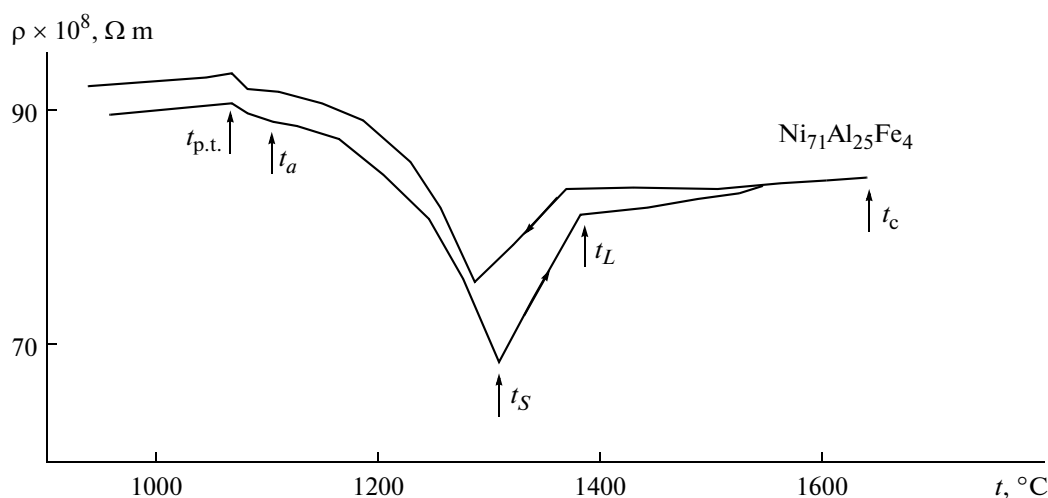


Fig. 2. Temperature dependence of resistivity of the  $\text{Ni}_{71}\text{Al}_{25}\text{Fe}_4$  alloy. Arrows on the curves show heating and cooling.

Resistivity for all alloys under study increases monotonically as the temperature increases and then decreases, after which it increases again. A characteristic dependence is shown in Fig. 2 by the example of the  $\text{Ni}_{71}\text{Al}_{25}\text{Fe}_4$  alloy. A similar run of  $\rho(t)$  for the  $\text{Ni}_3\text{Al}$ -based intermetallic alloys is found in [14].

For alloys in which iron atoms substitute aluminum, a decrease in  $\rho$  upon heating in the solid state is associated with the dissolution of the  $\gamma'$  phase at temperatures below  $t_a$ .

The alloys in which the iron atoms occupy nickel and aluminum sites differ from the previous group by the fact that a single-phase  $\gamma'$  state is retained to high temperatures. Therefore, the disordering onset is initially fixed in polytherms, and then the dissolution of the  $\gamma'$  phase is observed.

Let us note the ambiguity of the influence of iron on the character of processes in alloys with the substitution of nickel sites. The  $\text{Ni}_{73}\text{Al}_{25}\text{Fe}_2$  alloy is almost a single-phase intermetallic compound (the content of the  $\beta$  phase <1%). The only transition, which is fixed upon heating, is the disordering onset. An increase in the iron concentration to 4% (the  $\text{Ni}_{71}\text{Al}_{25}\text{Fe}_4$  alloy) leads to varying the sequence of processes. In this case the  $\gamma'$  phase initially dissolves and disordering is imposed with a further increase in temperature.

It should be noted that, with alloying into the nickel site, the alloys melt with the participation of the  $\beta$  phase ( $\text{NiAl}$ ). The phase composition of the  $\text{Ni}_{73}\text{Al}_{25}\text{Fe}_2$  alloy in the melting instant is  $\beta + \gamma'$ . The  $\text{Ni}_{71}\text{Al}_{25}\text{Fe}_4$  alloy has another phase composition, namely,  $\beta + \gamma$ . We failed to reveal the transition from the two-phase  $\gamma + \gamma'$  region into the three-phase  $\beta + \gamma + \gamma'$  region by the DTA data (Fig. 1a). It seems likely that the temperature range of the three-phase region was smaller than the measurement accuracy.

Figure 3 shows the influence of alloying with iron on the disordering onset temperature ( $t_a$ ) of alloys under study allowing for the measurement accuracy

of  $\pm 10^\circ\text{C}$ . The authors of [15] determined  $t_a = 1330^\circ\text{C}$  for the  $\text{Ni}_3\text{Al}$  intermetallic compound (composition 75.3 at % Ni, 24.7 at % Al), which we used as the reference point. As the iron content increases, magnitude  $t_a$  decreases (Fig. 3). These results correlate well with the data of review [6]. Alloying determines at least an increase in the concentration of the alloying element and the transition from the properties of the intermetallic compound to the properties of the ordering alloy. The substitution of nickel sites with iron leads to a considerable decrease in the temperature of the disordering onset.

With the further heating of the studied alloys, the range of melting of intermetallic compounds  $t_s - t_L$  with the jumplike increase in resistivity is observed (Fig. 2). After the complete melting of the samples, the intensity of increasing  $\rho$  decreases by an order of magnitude. The subsequent cooling is accompanied by the hysteresis of polytherms of  $\rho$ ; i.e., heating and cooling branches do not coincide. A similar phenomenon was observed in other studies devoted to studying the intermetallic compounds, e.g., in [14].

Currently, the notion on the melt of the intermetallic compound like on the nonequilibrium microhomogeneous system is formed [9, 14]. The presence of nonequilibrium microgroupings of atoms with a short-range order of the  $\text{Ni}_3\text{Al}$  type in the liquid state, which inherit the elements of the structure of the starting solid phase, is characteristic of the  $\text{Ni}_3\text{Al}$ -based alloys. With a certain temperature  $t_c$ , which is called critical, the nonequilibrium microgroupings decompose and the melt comes into the equilibrium and microhomogeneous state. It is retained with the subsequent cooling and leads to the hysteresis phenomenon of polytherms of  $\rho$ . The values of  $t_c$  of the studied  $\text{Ni}_3\text{Al}-\text{Fe}$  alloys are presented in the table.

It should be noted that the absence of hysteresis was observed in the case when heating of the melt was finished at temperatures below  $t_c$  [9].

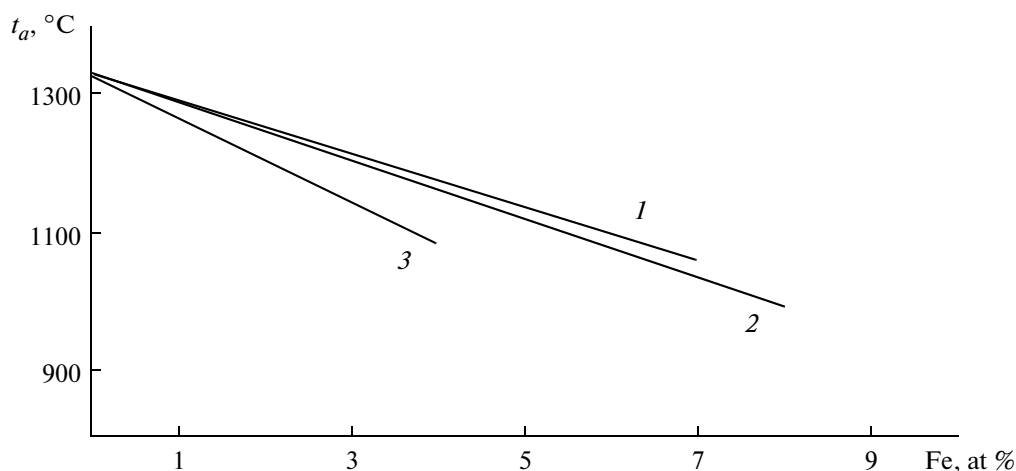


Fig. 3. Influence of iron alloying on the temperature of the disordering onset in the Ni<sub>3</sub>Al–Fe alloy. (1) Alloying in the aluminum atomic sites, (2) alloying into the aluminum and nickel atomic sites simultaneously, and (3) alloying into the nickel sites.

The state of the melt substantially affects the crystallization processes [9]. This is particularly confirmed by our data. After heating to  $t_c$ , range  $t_S$ – $t_L$  narrowed with the subsequent cooling (table).

### CONCLUSIONS

Using the measurements of the temperature dependence of resistivity in a broad temperature range (including the liquid state) and differential thermal analysis, the temperatures of phase transformations for the series of the Ni<sub>3</sub>Al–Fe alloys of various compositions are established in the homogeneity limits of the  $\gamma'$  phase. Temperatures of disordering onset ( $t_a$ ) are determined for all compositions.

(i) The magnitude of  $t_a$  is determined upon heating in resistivity polytherms. It decreases as the iron content increases. As the iron concentration increases, doping leads to the transition from the properties of the intermetallic compound to the properties of ordering alloy. The substitution of nickel atomic sites with iron determines the considerable decrease in temperature  $t_a$ .

(ii) The hysteresis phenomenon is observed in the liquid state in polytherms of  $\rho$  upon heating the samples under study to critical temperature  $t_c$ . The hysteresis of resistivity is associated with the elimination of the inherited influence of the structure of the starting solid sample on the melt structure and with the transition of the system into the more equilibrium and microhomogeneous state.

### ACKNOWLEDGMENTS

This study was supported by the Concourse for Research Works of Young Scientists at the Ural Federal University and partially supported by the Program of the Presidium of the Russian Academy of Sciences no. 12-U-2-1017.

### REFERENCES

1. Kablov, E.N. and Golubovskii, E.R., *Zharoprochnost' nikel'nykh splavov* (Heat Resistance of Nickel Alloys), Moscow: Mashinostroyeniye, 1998.
2. Stoloff, N.S., *Inter. Mater. Rev.*, 1989, vol. 34, no. 4, p. 153.
3. Povarova, K.B., Bazyleva, O.A., Drozdov, A.A., et al., *Materialovedenie*, 2011, no. 4, p. 39.
4. Savin, O.V., Stepanova, N.N., Akshentsev, Yu.N., et al., *Fiz. Met. Metalloved.*, 1999, vol. 88, no. 4, p. 69.
5. Cahn, R.W., Siemers, P.A., Geiger, J.E., and Bardhan, P., *Acta. Metall.*, 1987, vol. 35, no. 11, p. 2737.
6. Kozubski, R., Soltys, J., Cadeville, M.C., et al., *Intermetallics*, 1993, vol. 1, p. 139.
7. Syutkina, V.I., Kislitsina, I.E., Abdulov, R.Z., and Rudenko, V.K., *Fiz. Met. Metalloved.*, 1986, vol. 61, no. 3, p. 504.
8. Los', V.F., Repetskii, S.P., and Garkusha, V.V., *Metallofizika*, 1991, vol. 13, no. 9, p. 28.
9. Baryshev, E.E., Tyagunov, G.V., and Stepanova, N.N., *Vliyaniye struktury rasplava na svoystva zharoprochnykh nikel'nykh splavov v tverdom sostoyanii* (Influence of the Melt Structure on the Properties of Heat-Resistant Nickel Alloys in the Solid State), Yekaterinburg: Ural Branch Russ. Acad. Sci., 2010.
10. Lepikhin, S.V., Stepanova, N.N., Akshentsev, Yu.N., et al., *Fiz. Met. Metalloved.*, 2004, vol. 97, no. 4, p. 88.
11. Kazantseva, N.V., Vinogradova, N.I., Stepanova, N.N., et al., *Fiz. Met. Metalloved.*, 2009, vol. 107, no. 4, p. 401.
12. Tyagunov, G.V., Baum, B.A., Tsepelev, V.S., et al., *Zavod. Lab. Diagnost. Mater.*, 2003, vol. 69, no. 2, p. 35.
13. Lepikhin, S.V., Baryshev, E.E., Tyagunov, G.V., et al., *Zavod. Lab. Diagnost. Mater.*, 2005, vol. 71, no. 4, p. 35.
14. Nikolaev, B.V. and Tyagunov, G.V., *Rasplavy*, 1995, no. 4, p. 22.
15. Savin, O.V., Stepanova, N.N., Akshentsev, Yu.N., et al., *Fiz. Met. Metalloved.*, 2000, vol. 90, no. 1, p. 66.

Translated by N. Korovin